



## Analyses for various doping structures of SOI-based optical phase modulator using free carrier dispersion effect

B. Mardiana<sup>a,b,\*</sup>, Sahbudin Shaari<sup>a</sup>, P. Susthitha Menon<sup>a</sup>, H. Hazura<sup>a,b</sup>,  
A.R. Hanim<sup>a,b</sup>, N. Arsad<sup>a</sup>, H. Abdullah<sup>a</sup>

<sup>a</sup> Institute of Microengineering and Nanoelectronics, Universiti Kebangsaan Malaysia, 43600 UKM Bangi, Malaysia

<sup>b</sup> Faculty of Electronic and Computer Engineering, Universiti Teknikal Malaysia Melaka (UTeM), Hang Tuah Jaya, 76100 Durian Tunggal, Melaka, Malaysia

### ARTICLE INFO

#### Article history:

Received 30 April 2013

Accepted 16 September 2013

Available online xxx

### ABSTRACT

This paper highlights the study on various structure of silicon-on-insulator (SOI) optical phase modulators based on free carrier dispersion effect. The proposed modulators employ the forward biased P-I-N diode structure integrated in the waveguide and will be working at 1.55  $\mu\text{m}$  optical telecommunications wavelength. Three kinds of structure are compared systematically where the p+ and n+ doping positions are varied. The modeling and characterization of the SOI phase modulators was carried out by 3D numerical simulation package. Our results show that the position of doping regions have a great influences to the device performance. It was discovered that the best structure in this work demonstrated modulation efficiency of 0.015 V cm with a length of 155  $\mu\text{m}$ .

© 2013 Published by Elsevier GmbH.

### 1. Introduction

Recently, silicon-on-insulator (SOI) based optical modulator have earned an evolving interest due to its significant role in the inter-chips optical interconnect. Silicon-on-insulator (SOI) substrates are widely used to fabricate optoelectronic devices due to the high index contrast between the silicon core and the silica cladding [1]. Furthermore, silicon has proven to be a relatively cheaper material compared to other III–V semiconductor materials and suitable for integrated photonic system. In addition, SOI has significant advantages in which it has very low bending loss [2]. Therefore, more compact device can be materialized with the utilization of SOI as the substrate material [3].

Phase modulator are used to change the data signal from electrical domain to optical domain. The most effective way to modulate the signal in silicon-based modulator is by free carrier dispersion effect. This mechanism is used due to the facts that unstrained pure crystal silicon does not have electro-optic effect such as Pockels effect, Kerr effect and Franz–Keldysh effect [4]. To create the free carrier dispersion effect in silicon modulator, the electrical structure has been either a P-I-N diode in injection mode, a PN diode in depletion mode or with the use of MOS capacitor. The carrier injection P-I-N diode structure is widely implemented as electrical

structure of modulator due to its high efficiency and smallest size [5].

In this paper, the P-I-N SOI phase modulators are designed in three structures with different kind of doping positions. The three-dimensional (3D) semiconductor simulation package SILVACO was used for this purpose. In this paper, the 3D designs are utilized because of the designs consider the doping positions variations in the in z-axis. Therefore, the dispersion effect of free carrier electrons and holes can be examined along z-axis.

### 2. Theory

The modeling of the optical modulator was performed using a commercial numerical simulator 3D-SILVACO which employ a drift-diffusion approach [6]. The Poisson, carrier continuity and current density equations are solved numerically in three dimensions subject to the device's geometry and boundary conditions imposed by the device's contacts and biasing conditions. The basic equation to be solved at each node during a simulation tool is given by the Poisson equation:

$$\nabla(\epsilon \nabla \psi) = -q[n - p + \Sigma(N_A^- - N_D^+ + N_{AA}^- - N_{DD}^+)] \quad (1)$$

where  $\psi$  is the electrostatic potential,  $\epsilon$  is epsilon,  $q$  is the electronic charge,  $n$  and  $p$  is the density of movable carriers,  $N_A^-$  and  $N_D^+$  are respectively the concentration of ionized donors and recipients respectively while the  $N_{AA}^-$  and  $N_{DD}^+$  is the concentration of traps carrier that serves as the recipient and donor ionized.

The modulators operation is modeled by taking into account the carrier generation in optical and thermal, recombination process

\* Corresponding author at: Institute of Microengineering and Nanoelectronics, Universiti Kebangsaan Malaysia, 43600 UKM Bangi, Malaysia.

E-mail address: [mardiana@utem.edu.my](mailto:mardiana@utem.edu.my) (B. Mardiana).

and the process of carrier drift and diffusion. Continuity equation for the electron and hole carriers describes the relationship between these processes and is given by;

$$\frac{\partial n}{\partial t} = G_n - R_n + \frac{1}{q} \nabla \cdot \vec{J}_n \quad (2)$$

$$\frac{\partial p}{\partial t} = G_p - R_p + \frac{1}{q} \nabla \cdot \vec{J}_p \quad (3)$$

where  $G_n$  and  $G_p$  which is the rate of production of electrons and holes resulting from external effects such as optical excitations in high-energy photons, while  $J_n$  and  $J_p$  are the electron and hole current density.  $R_n$  and  $R_p$  is the carrier recombination rate.

Generally, current flow occurs in the combined process of diffusion and drift in the presence of an electric field. Current density for electrons and holes,  $J_n$  and  $J_p$  is given by the drift-diffusion model as;

$$\vec{J}_n = q\mu_n n \vec{E} + qD_n \vec{\nabla} n \quad (4)$$

$$\vec{J}_p = q\mu_p p \vec{E} + qD_p \vec{\nabla} p \quad (5)$$

where  $D_n$  and  $D_p$  is the diffusion constant of electrons and holes,  $\mu_n$  and  $\mu_p$  are the electron and hole mobility and  $E$  is the electric field.

Next, a brief explanation of the phase modulation mechanism of the proposed modulator is given here to express the idea of the proposed device operation. Phase modulator fabrication is done by incorporating complementary metal-oxide semiconductor (CMOS) technology. The electrons and holes will move through the channel as voltage is supplied. The carrier concentration at in the waveguide is measure based on the value of carrier concentration. The following equation expresses the calculation of refractive index change and free carrier absorption loss at 1.55  $\mu\text{m}$  wavelength due to free carrier injection of the device [11]: the change of refractive index,  $\Delta n$  can be calculated [7]:

$$\Delta n = -(8 \times 10^{-22} \Delta N_e + 8.5 \times 10^{-18} (\Delta N_h)^{0.8}) \quad (6)$$

$$\Delta \alpha = 8.5 \times 10^{-18} \Delta N_e + 6 \times 10^{-18} \Delta N_h \quad (7)$$

where  $\Delta N_e$  is the change of the free electrons concentration and  $\Delta N_h$  is the change of the free hole concentration. Then, the propagating optical mode,  $\Delta n$  is calculated from the equation [8]:

$$\Delta \varphi = 2\pi n L_\pi / \lambda_0 \quad (8)$$

where  $L_\pi$  is length of the active region of the modulator and  $\lambda_0$  is optical wavelength.

$$L_\pi = \lambda_0 / 2\Delta n \quad (9)$$

### 3. Methodology

In this paper, the structure is based on a P-I-N lateral optical phase modulator fabricated on silicon-on-insulator (SOI) substrate [9]. The models were developed using the Athena and Devedit module in Silvaco. The fabrication processes begin with the formation of the SOI layer. Then, the silicon layer is lightly doped with a background concentration of  $1 \times 10^{14} \text{ cm}^{-3}$ . The rib waveguide is formed using the etching process where an oxide layer is used as a mask. The rib height and width for the waveguide structure specified to obtain single mode behavior. The rib structure is designed to have 0.46  $\mu\text{m}$  in slab height ( $h$ ) and 0.4  $\mu\text{m}$  in rib width ( $W$ ). The active area of p-i-n diode structure was fabricated through the ion implantation process where both the  $p^+$  and  $n^+$  region were implanted with boron and phosphorus respectively. The  $p^+$  type region was doped with boron concentration of  $5 \times 10^{19} \text{ cm}^{-3}$  at ion

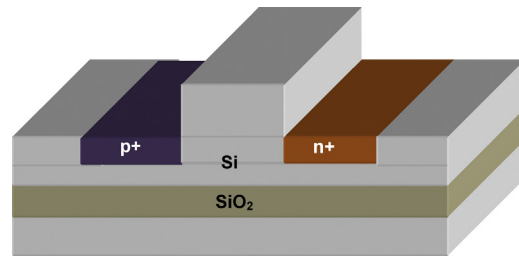


Fig. 1. The first structure with one pair of wells next to the waveguide rib.

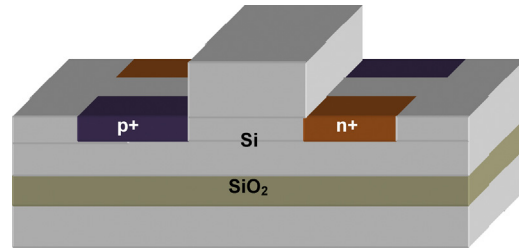


Fig. 2. The second structure with two pairs of wells next to the waveguide rib.

implantation energy of 10 keV and annealing temperature of 600 °C. While the  $n^+$  type region was doped with phosphorous concentration of  $5 \times 10^{19} \text{ cm}^{-3}$  at ion implantation energy of 30 keV and annealing temperature of 600 °C. Finally, the metallization process was done to form the electrodes of anode and cathode.

Three different structures of SOI phase modulator were designed and studied in this work. In the first structure, only one pair of  $p^+$  and  $n^+$  wells existed adjacent to the waveguide rib as shown in Fig. 1. Fig. 2 shows the second structure where 2 pairs of wells were placed at the region next to the rib waveguide. Finally in the third structure as shown in Fig. 3, in addition to the two pairs of wells, an additional two pairs of doped wells were placed on the waveguide rib.

### 4. Results and discussion

Prior to electrical characterization, the optical analysis was carried out by using FDTD simulation to ensure the single mode behavior of the proposed device. Fig. 1 shows the TE fundamental mode profile of the proposed device at wavelength 1.55  $\mu\text{m}$ . It is proven that the single mode behavior was obtained as calculated (Fig. 4).

The performance of the silicon phase modulators were evaluated by varying the positions of the  $n^+$  and  $p^+$  doping regions. The effect of doping regions position will be investigated based on total free carrier concentration, refractive index change, free carrier absorption loss, size and the modulation efficiency of the modulators.

Fig. 5 shows the carrier concentration of free electrons and holes of the three different structures of modulators when specific

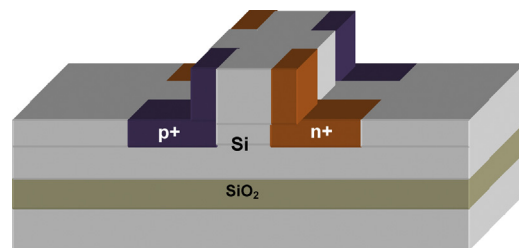


Fig. 3. The third structure with additional doped wells on the rib waveguide.

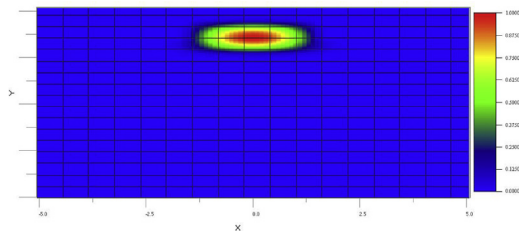


Fig. 4. Total free carrier concentration against applied voltage.

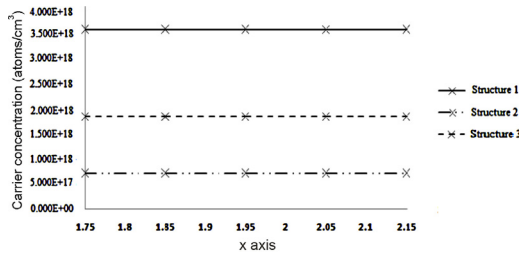


Fig. 5. Total free carrier concentration along x-axis.

voltage is applied. The measurement of free electrons and holes was taken along x axis from  $x=1.75$  to  $x=2.15$  which is the area of optical mode propagate in the device. It is clearly seen that structure 1 and structure 3 gave higher density of free carrier compare to structure 2. This happened due to interdigitated doping position of  $p^+$  dan  $n^+$  region in structure 2 and structure 3 cause free electrons and holes to move in many directions instead of one direction as in structure 1. Therefore, the existing of free electrons and holes in the optical mode guiding region are reducing. The results proof that the concentration of existing free carrier in the active region can be manipulated by the position of doping region  $n^+$  and  $p^+$ . Thus, the determination of doping positions are very important in designing the P-I-N SOI phase modulator because it will influence the way how the free electrons and holes move in the active region of the device.

Fig. 6 shows the relationship between drive voltage and the refractive index change ( $\Delta n$ ) at  $1.55 \mu\text{m}$  wavelength. In general, the total refractive index change ( $\Delta n$ ) increases as the applied voltage is higher. For instance in structure 1, by varying the applied voltage from 0.7 V to 1 V caused almost 0.005 changes in refractive index of the waveguide. This happened due to more injected free holes and electrons moved from the doping region to the optical guidance area when more applied voltage was supplied. Thus, this scenario causes the increase in the free carrier density and resulting improvement of refractive index change ( $\Delta n$ ) in the guidance region of the device. It is found that, the structure 1 has the largest effect on the refractive index change ( $\Delta n$ ), followed by the structure 3 and the structure 2.

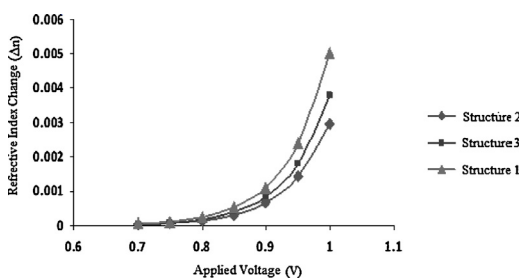


Fig. 6. Refractive index change for phase modulators with various waveguide structures.

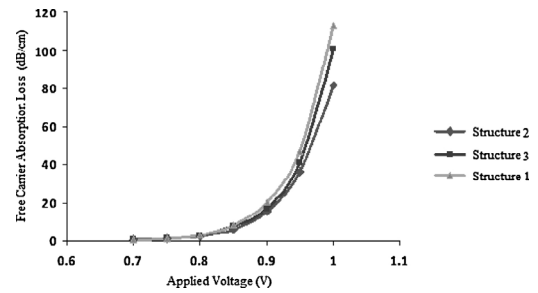


Fig. 7. Free carrier absorption loss for phase modulators with various waveguide structures.

Table 1  
Modulation efficiency and length of modulator.

Structure	1	2	3
Length (cm)	0.0155	0.0261	0.0205
Modulation Efficiency (V cm)	0.013	0.023	0.018

Fig. 7 shows the comparison of the absorption losses value with various structure of SOI P-I-N phase modulators. The results indicated that, upon increasing the drive applied voltage, the absorption loss increased gradually. Structure 1 produced highest free absorption loss compared to structure 2 and structure 3. Even though structure 1 is proven to have the highest refractive index change ( $\Delta n$ ) in the previous section but this structure is suffering from biggest absorption loss ( $\Delta \alpha$ ). Therefore, in seeking a balanced response between the high refractive index change and low free carrier absorption loss, a design trade off between the two is needed in order to produce a good SOI phase modulator.

Table 1 shows the comparison of estimated length and the modulation efficiency. The modulation efficiency is a very important parameter for characterizing the modulator performance and its value can be determined by overlapping the modulation region with the optical field. The optimized interactive length of various structures of phase modulators investigated in this work is obtain from the value of refractive index change ( $\Delta n$ ) in Fig. 6 and calculated from Eq. (9). The modulation efficiency can be predicted by Figure of Merit (FoM)  $V_{\pi}L_{\pi}$ , where  $V_{\pi}$  is the voltage to achieve a  $\pi$  phase shift. The lower the value of this FoM, the more efficient the modulator is. Result shows that a smallest device can be realized with structure 1 and resulting the best modulation efficiency of 0.00018 V cm. As a comparison, the modulation efficiency of structure 1 is 50% better than structure 3% and 82% better than structure 2.

## 5. Conclusion

The SOI phase modulators based on P-I-N diode structure has been modeled using a 3D SILVACO simulation package. We have analyzed the performance of modulators with various structure of doping positions. We have shown that doping positions of  $n^+$  and  $p^+$  can be used to manipulate the density of free electrons and holes in a device. In seeking a balanced response between the high refractive index change and carrier absorption loss, a design trade off between the two is needed to be taken into consideration depending on the application of the modulator.

## Acknowledgments

The authors would like to acknowledge Universiti Teknikal Malaysia Melaka (UTeM) for the support. This research is financially supported by the Ministry of Higher Education of Malaysia and Universiti Kebangsaan Malaysia (UKM).

**References**

- [1] A.S. Liu, L. LiO, D. Rubin, H. Nguyen, B. Ciftcioglu, Y. Cherit, N. Izhaky, M. Paniccia, High-speed optical modulation based on carrier depletion in a silicon waveguide, *Opt. Express* 15 (2007) 660–668.
- [2] C.A. Barrios, M. Lipson, Electrically driven silicon resonant light emitting device based on slot-waveguide, *J. Appl. Phys.* 96 (2005) 6008–6015.
- [3] C.E. Png, S.P. Chan, S.T. Lim, G.T. Reed, Optical phase modulators for MHz and GHz modulation in silicon-on-insulator (SOI), *J. Lightwave Technol.* 22 (2004) 1573–1582.
- [4] C. Li, L. Zhou, A.W. Poon, Silicon microring carrier-injection-based modulators/switches with tunable extinction ratios and OR-logic switching by using waveguide cross-coupling, *Opt. Express* 15 (2007) 5069–5076.
- [5] G.T. Reed, A.P. Knights, *Silicon Photonics – An Introduction*, John Wiley & Sons, UK, 2004.
- [6] F.Y. Gardes, D.J. Thomson, N.G. Emerson, G.T. Reed, 40 Gb/s silicon optical modulators, *Opt. Express* 12 (2011) 11804–11813.
- [7] H. Xu, X. Xiao, X. Li, Y. Hu, Z. Li, T. Chu, Y. Yu, J. Yu, High speed silicon Mach-Zehnder modulator based on interleaved PN junctions, *Opt. Express* 20 (2012) 15093–15099.
- [8] B. Mardiana, A.R. Hanim, H. Hazura, S. Shaari, P.S. Menon, H. dan Abdullah, Active SOI optical ring based on free carrier injection, *J. Adv. Mater. Res.* 403–408 (2012) 758–761.
- [9] M. Ziebell, D.M. Morini, G. Rasigade, J.M. Fédéli, P. Crozat, E. Cassan, D. Bouville, L. Vivien, High-speed ring resonator silicon optical modulator based on interleaved PN junctions, *Opt. Express* 20 (2012) 10591–10596.
- [11] Q. Xu, S. Manipatruni, B. Schmidt, J. Shakya, M. Lipson, All-optical logic based on silicon micro-ring resonators, *Opt. Express* 15 (2007) 430–436.